Development of Helium Electron Cyclotron Wall Conditioning on TCV for the operation of JT-60SA

D. Douai[1], T. Goodman[2], A. Isayama[3], M. Fukumoto[3], T. Wauters[4], C. Sozzi[5], S. Coda[2], P. Blanchard[2], L. Figini[5], S. Garavaglia[5], Y. Miyata[3], A. Moro[5], D. Ricci[5], M. Silva[2], C. Theiler[2], S. Vartanian[1], K.Verhaegh[2], the EUROfusion MST1 Team*, the TCV Team

[1]CEA, IRFM, F-13108 St-Paul-Lez-Durance, France
[2] Ecole Polytechnique Fédérale de Lausanne (EPFL), Swiss Plasma Center (SPC), CH-1015 Lausanne, Switzerland
[3]National Institutes for Quantum and Radiological Science and Technology, Naka, Ibaraki 311-0193, Japan
[4]Laboratory for Plasma Physics, ERM/KMS, 1000 Brussels, Belgium, TEC Partner
[5]Istituto di Fisica del Plasma CNR, Milano, Italy
* See appendix of H. Meyer et.al. (OV/P-12) Proc. 26th IAEA Fusion Energy Conf. 2016, Kyoto, Japan

E-mail contact of main author: david.douai@cea.fr

Abstract. JT-60SA envisions Electron Cyclotron Wall Conditioning (ECWC), as wall conditioning method in the presence of the toroidal field to control fuel and impurity recycling and to improve plasma performance and reproducibility. This paper reports on Helium ECWC experiments on TCV in support of JT-60SA operation. Nearly sixty Helium conditioning discharges have been successfully produced in TCV, at a toroidal field B_T = 1.3 or 1.54 T, with gyrotrons at 82.7 GHz in X2 mode, mimicking ECWC operation in JT-60SA at the second harmonic of the EC wave. Discharge parameters were tuned in order to (i) minimize the time for the onset of ECWC plasmas, thus minimizing absorption of stray radiation by in-vessel components, (ii) improve discharge homogeneity by extending the discharge vertically and radially, and wall coverage, in particular of inboard surfaces where JT-60SA plasmas will be initiated, (iii) assess the efficiency of He-ECWC to deplete carbon walls from fuel. An optimized combination of vertical and radial magnetic fields, with amplitudes typically 0.1 to 0.6% of that of B_T, has been determined, which resulted in lowest breakdown time, improved wall coverage and enhanced fuel removal. A standard ohmic D_2-plasma could be then sustained, whereas it wouldn't have been possible without He-ECWC.

1. Introduction

During the initial research phase of the fully superconducting large tokamak JT-60SA, with divertor targets made of carbon-fibre composite (CFC), but also in its planned operation with phased increase of metallic divertor targets [1], wall conditioning will be required to control fuel and impurity recycling and to improve plasma performance and reproducibility. Wall conditioning will occur either before plasma operation after torus vacuum vessel openings, or during operation, between plasma pulses, for reliable discharge initiation, control of fuel recycling or recovery after disruptions. In JT-60SA, the toroidal magnetic field, generated by superconducting coils, will be continuously maintained. In the presence of such a magnetic field, conventional DC-glow discharges are unstable and can therefore no longer be used between plasma pulses. Compatible with the magnetic field, Taylor Discharge Cleaning (TDC) has been developed and routinely used with B_T on between plasmas in JT-60U to recover a satisfactory wall pumping capacity or low impurity levels, for instance after a disruption [2], [3]. These short low current plasmas, typically with duration of 20-40 ms and a current of a few tens of kA, are created inductively in the vacuum vessel by rapidly changing the currents in the central solenoid coil, at a repetition rate of ~0.2-1 Hz. However, TDC will

not be available anymore in JT-60SA, where the rate at which coil currents can be changed in the superconducting poloidal field coils will be limited.

Electron Cyclotron Wall Conditioning (ECWC) plasmas can be easily produced in the presence of the toroidal magnetic field using ECRF wave launchers and are therefore envisioned, for reliable discharge initiation, recovery after disruptions, and/or desaturation of carbon walls from fuel in JT-60SA [1]. ECWC has been successfully operated in Helium at the first harmonic in JT-60U, allowing recovering from disruptions [4]. However, in JT-60SA (R = 2.96 m, a = 1.18 m, B_T between 1.72 and 2.25 T, depending on the operation scenario), with gyrotron frequencies f = 110 or 138 GHz, ECWC discharges will have to be operated at the second harmonic of the EC wave.

Localized power deposition in ECWC plasmas can however affect discharge uniformity and cleaning efficiency of ECWC, especially at the 2nd harmonic. With low absorption in X2 mode, ECWC discharges at second harmonic are known to be less homogeneous than at first harmonic (see e.g. [5] or [6]), Indeed, ionization occurs preferentially at the intersection of the EC beam and the ECR surface at $\omega = n \cdot q \cdot B_T \cdot (R)/m_e$, with q the charge of the electron, m_e its mass and n = 2, resulting in poor discharge uniformity, small wetted area and interaction with inner wall surfaces. Discharge homogeneity can be improved by the application of a weak poloidal field, and several attempts aiming at extending the discharge radially by superposing a weak (<1% of B_T) horizontal magnetic field have been reported [4], [6]. A recent paper [7] evidenced however in JT-60U a lower conditioning efficiency in ECWC discharges at second harmonic than in X1-mode, but there is up to now no demonstration of the effectiveness of ECWC at the second harmonic for the operation of a tokamak, i.e. of its ability to efficiently clean wall surfaces for reliable plasma initiation or recovery from disruption.

This paper reports on Helium 2nd harmonic ECWC experiments on TCV in support of JT-60SA operation, with the aim to develop and optimize the technique, to assess its efficiency and to demonstrate its reliability for wall desaturation. The experiment performed in TCV is described in a first part. Experimental results on plasma production, homogeneity and finally efficiency for fuel removal are presented in a second one. Finally we present conclusions on the feasibility of ECWC at the second harmonic as a wall conditioning technique in JT-60SA.

2. ECWC operation in TCV

Discharges are operated in TCV (R = 0.88 m, a = 0.25 m, with carbon PFCs) at a toroidal field B_T = 1.3 or 1.54 T, in X2 mode with up to simultaneously two of its three gyrotrons at 82.7 GHz. Two of the used launchers (Antennas 2 and 6 in sectors 2 and 7 resp., see FIG. 1) are located in the upper mid-plane, toroidally spaced by 120°, whereas a third one (Antenna 4 in sector 6) is in the midplane. Given the fields and frequency at which discharges were operated, the cold 2nd harmonic ECR layer lies in TCV at ρ = -0.4 or 0.15, with ρ = r/a the normalized radius (-1 ≤ ρ ≤ 1), mimicking operation in JT-60SA at 110 GHz (ρ = -0.31 at B_T = 1.72 T and ρ = 0.36 at B_T = 2.25 T). Antennae 2 and 6, located at an angle of 120 degrees each from the other in the toroidal direction, as well as antennae 6 and 4, have been operated alternately and neither toroidal nor poloidal asymmetry could be detected.

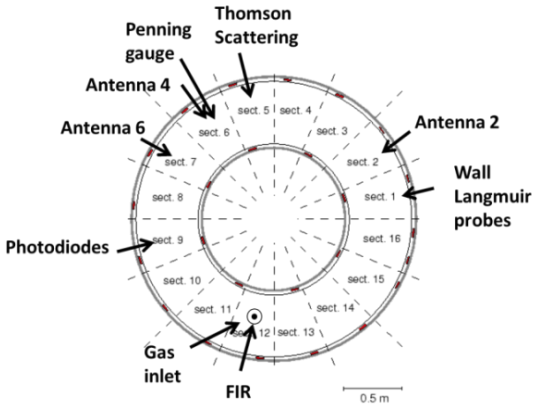

FIG. 1. Top view of TCV, with positions of ECRH antennas and diagnostics used for the ECWC experiment.

Toroidal and poloidal injection angles were typically 5 and -10°, although larger poloidal angles have been tested.

Fifty seven successful discharges have been produced in TCV, in two experimental sessions, with durations of 1.5 or 2 sec., such as the one shown in FIG. 2, with the aim to maximize wall release vs. pressure, power and poloidal field. Helium was injected through one of the piezoelectric valves at the bottom of the device, and exhausted (with Deuterium released from the walls) by the four turbo-molecular pumps of TCV, located at mid-plane, with a total nominal pumping speed of 4 $m^3 \cdot s^{-1}$. Gas was inlet at t = -4.0 sec., yielding a stable pressure ranging between $5 \cdot 10^{-3}$ and $2 \cdot 10^{-2}$ Pa before the discharge. At t = 0.2 sec., ECRH was injected for 2 sec., with powers between 90 and 480 kW. Scaled to the area of the inner walls of JT-60SA (100 m^2), this would hence result in ECRH powers between 1 and 5 MW, assuming the same operating pressure.

Different poloidal field patterns have been used in TCV, using its sixteen shaping coils distributed at low and high field sides, with the aim to extend the discharge vertically and radially. Since in JT-60SA, plasmas will be initiated in limiter configurations attached to inboard wall surfaces, conditioning discharges with the largest radial extension and subsequent interaction with inboard wall surfaces have been particularly targeted in TCV. Poloidal field patterns were either computed before the experiment, in order to set currents to the coils, or reconstructed afterwards, from plant values. Hence, poloidal fields with amplitudes ranging from 0.1 to 2% of B_T at $\rho = 0$ have been tested.

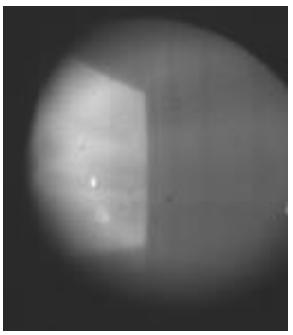

FIG. 2. CCD image of a ECWC plasma in TCV (pulse 51551, $p=10^{-2}$ Pa, P_{ECRH}=480kW).

Discharge homogeneity was estimated from the electron density radial profile measured with Far Infrared Interferometry (FIR) and from visible CCD images, while wall coverage was assessed from the ion saturation current measured by the TCV array of wall-mounted Langmuir probes located at the high and low field sides, and at the bottom of the device. Electron densities of $15 \cdot 10^{18}$ m^{-3} and temperatures of 20-40 eV have been measured with the TCV FIR and/or Thomson Scattering systems. Typical edge temperatures were found to be 3 eV at the probes.

Since ECWC discharges are low density and optically thin plasmas, single pass absorption of EC wave is low, leading to EC wave reflection and stray radiation, especially before breakdown. Breakdown conditions were therefore optimized against gas pressure, power and poloidal field pattern. TCV pyroelectric detectors were used to detect any stray radiation occurring during the discharges.

The efficiency of He-ECWC was assessed from the amount of released D_2 fuel, using an optical Penning gauge (Alcatel FA111) connected to the vacuum vessel. The emitted light from the gas ionized in the gauge was sent to a mirror-based (Schmidt-Czerny-Turner) spectrometer (Princeton Instruments Isoplane SCT 320). Intensities of the emitted lines at 6561.03 Å for D_α and 6678.1 for He I were calibrated in dedicated shots against pressure, measured by a capacitance gauge (Baratron) nearby.

In TCV, 30 min. He-GDC are necessary and routinely operated to obtain the first plasma at the start of each experimental day. In order to assess the ability of He-ECWC to desaturate carbon wall surfaces of TCV, He-GDC were operated neither before nor during the experimental sessions.

3. Results

3.1.Breakdown of ECWC plasmas

ECWC are optically thin plasmas, where single pass absorption of the EC wave is low. As the beam is injected into the neutral gas, a fraction of the ECR power is absorbed by the electrons at the location of the ECR resonance, while the remaining power is reflected by the facing wall surfaces, diffused, de-polarized and damped on in-vessel components and an undefined mixture of O- and X-mode polarization will fill the whole vessel [10]. For the safe operation of ECWC, it is thus important to ensure sufficient absorption of the ECR power in order to avoid exposure of in-vessel components or diagnostics to excessive stray radiation which may damage them. ECR power absorption is even lower at second harmonic than at fundamental frequency [10]. Given the steady state density and temperatures in that case, the quasi-optical beam-tracing code GRAY [8] predicts a fraction of absorbed power between 70 and 80%. However, in the avalanche and density build-up phases of ECWC, absorption may be as low as a few percent's. Neutral gas breakdown in ECWC discharges is therefore a critical phase, where operational parameters have to be properly chosen in order to either maximize absorption at breakdown or shorten the breakdown time.

FIG. 3 shows time traces of the D_α signal in a ECWC shot in TCV as a function of the applied horizontal magnetic field B_H. In the pure toroidal case, the breakdown time t_{Bd}, defined as the difference between the burst in the D_α emission at breakdown (measured far away from the antenna port) and the application of the EC power, was typically ~10-15 msec. and was reproducible. However, t_{Bd} significantly increased upon application of B_H, and could vary with its amplitude from 80 msec. up to 500 msec., above which the gyrotron power was stopped by a trigger sent by the pyroelectric detector [9]. For $B_H \sim 0.2\%B_T$, with $B_T = 1.54T$, t_{Bd} could vary arbitrarily between 90 and 450 msec., as seen on FIG. 3, and breakdown was even not possible for $B_H > 0.2\%B_T$.

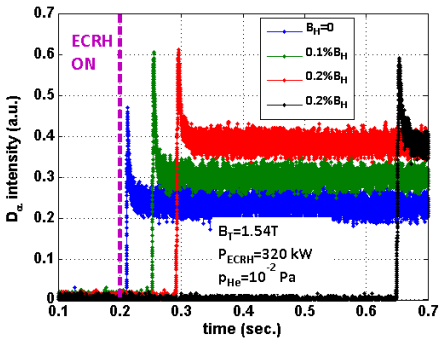

FIG. 3. D_α emission intensity for different amplitudes of the horizontal magnetic field B_H (blue: B_H = 0, green: B_H = 0.1%B_T, red and black: B_H = 0.1%B_T).

The breakdown time was measured for other discharge parameters. The results are shown in FIG.4. t_{Bd} was found to decrease with gas pressure, EC power and amplitude of the vertical field B_V. On the other hand, it was found larger at 1.3 T than at 1.54T, i.e. for the largest distance between the launcher and the ECR layer.

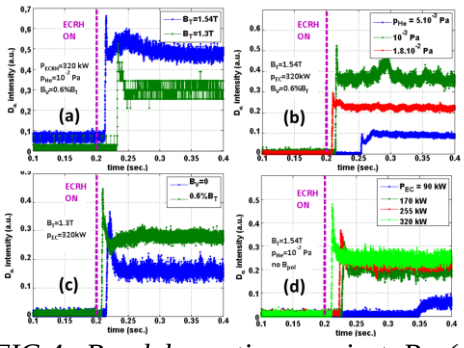

FIG.4. Breakdown time against B_T (a), pressure (b), B_V (c) and ECRH power (d).

3.2. Discharge homogeneity and wall coverage

As stated above, ECR power absorption is lower at second harmonic than at fundamental frequency. The few electrons created upon ionization of the neutral gas at the intersection of EC beam and ECR surface are rapidly lost to the walls, due to the vertical drift $\nabla B \times B$, and ECWC plasma production remains localized. Horizontal and vertical magnetic fields are thus required to extend the plasma radially and vertically. Whereas in the fundamental ECR scenario, a small horizontal field proved to extend discharge uniformity and plasma wetted area significantly, a more complex poloidal field

pattern is required to improve uniformity and wall coverage in ECWC discharges at the second harmonic [6].

On FIG. 5a are shown four electron density radial profiles, averaged over the EC pulse duration, in He-ECWC plasmas (B_T = 1.54 T, p = 10^{-2} Pa, P_{EC} = 320 kW) without poloidal field (blue), with B_H = 0.1% B_T (green), B_H = 0.2% B_T (red) and B_V = 0.6% B_T (black). Whereas the density sharply peaks near the ECR layer (dashed gray line) in the first case, the profiles tend to flatten upon application of the horizontal field, while density increases at the high field side, indicating a more homogeneous discharge in the horizontal direction. Moreover, density peaking slightly shifts inwards. Radial extension in the presence of B_H was confirmed by the relative variation of the ion saturation current j_{sat} measured by the wall Langmuir probes, which amplitude is illustrated in FIG. 5b as the distance of the blue dots to the neighbouring wall. The most interesting feature is the small increase of j_{sat} with B_H inboard, where plasmas are initiated in TCV and will be initiated in JT-60SA.

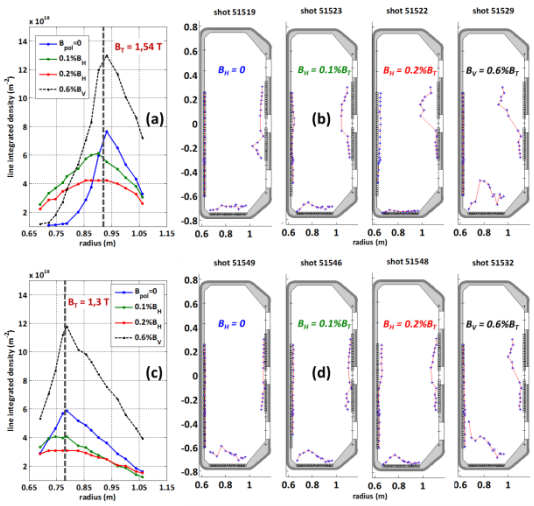

FIG. 5. Electron density radial profiles (a and c) and relative ion saturation current (b and d) in ECWC discharges ($p=10^{-2}$Pa, P_{EC}=320kW) for different values poloidal fields. Top: B_T=1.54T, bottom: B_T=1.3T.

The situation is similar at B_T = 1.3 T (FIG. 5c and d, same pressure and ECRH power), but the ECR layer being shifted inwards with respect to the case at B_T = 1.54 T, a slightly higher ion saturation current is measured inboard, with a decrease outboard. At 1.3 T, breakdown with B_H = 0.2%B_T was not possible, and the data were obtained from a shot with a ramp of B_H starting from of B_H = 0.05%B_T. At 1.54 T, in the case where a vertical field only is applied, density is increased by a factor two compared to the pure toroidal case, without any shift inwards of density peaking. Zero current was measured by the inboard wall Langmuir probes, but instead the probes indicated a strong interaction with both the divertor - a sign of vertical extension of the discharge - and the outboard limiter. Changing the toroidal field from 1.54 T to 1.3 T reduced the ion saturation current measured on the outboard limiters, but did not result in any increase of the ion flux on inboard surfaces.

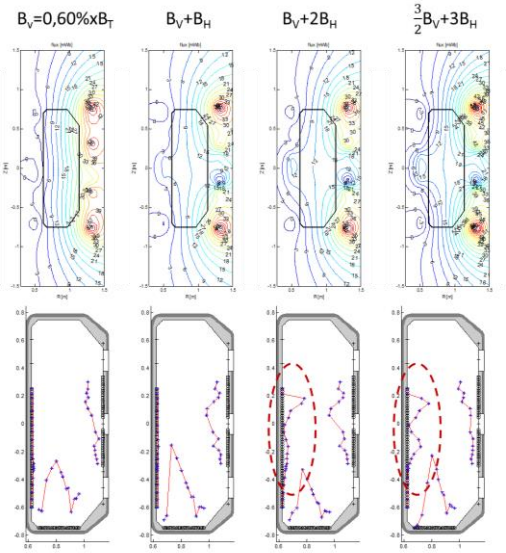

FIG. 6. Poloidal field patterns as reconstructed from plant values (top) and ion saturation currents from the wall Langmuir probes (bottom) for different combinations of B_H and B_V.

B_H and B_V were further adjusted in order to produce more uniform plasmas. FIG. 6 shows the magnetic flux patterns (top figures), as reconstructed from the values of the currents in the sixteen shaping coils of TCV, and the ion saturation currents (bottom) for different combinations of B_H and B_V in ECWC discharges at B_T = 1.3 T, p = 10^{-2} Pa, P_{EC} = 480 kW. The different plots in FIG. 6 are labelled B_V+B_H, B_V+2B_H and $\frac{3}{2}B_V$+3B_H, where $B_V \sim 0.6\%B_T$ and

$B_H \sim 0.1\%B_T$ in the equatorial plane. Starting from the pure vertical case, the radial component of the poloidal field was gradually increased using the shaping coils in the equatorial plane, bending there the vertical magnetic flux lines in and outboard, resulting in "barrel-shaped" patterns. Ion saturation could be measured inboard for $2B_H$ and was further increased as the radial component of the poloidal field B_H was increased. Largest currents on the inboard probes were obtained for shot 51960 with $\frac{3}{2}B_V+3B_H$. In all cases shown in FIG. 6, density profiles were similar to those of FIG. 5, but with plasma density peaks as large as $1.5 \cdot 10^{19}$ m^{-2} at the position of the resonance layer. Interestingly, all breakdown times were below 20 msec. with such combinations of poloidal fields.

3.3. Efficiency of ECWC

Helium and Deuterium partial pressures were measured with an optical Penning gauge during and after a He-ECWC discharge An illustration is given by FIG.7 which shows them as a function of time. He injection starts at t = -4.0 sec and is stabilized at t=0.2 sec. when the ECRH power is injected for 2 sec. In the case shown in FIG. 7, the He partial pressure is strongly depleted during the ECRH pulse, shown by the orange bar in FIG. 7, due to the confinement of the produced He^+ ions. During the discharge, D_2 is released from the walls, with a partial pressure measured to be at most 10% of the total pressure. D_2 is in fact mainly released by outgassing from the carbon walls after the discharge. For each ECWC discharge, the amount of fuel released and pumped out was calculated by integrating the Deuterium partial pressure multiplied by the pumping speed over the ECRH pulse duration and about 60 sec. post-discharge. Over both discharge and post-discharge phases, the amount of D_2 released could represent up to 30% of that of the He injected.

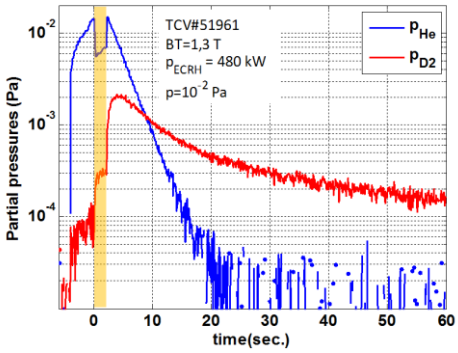

FIG. 7. He (blue) and released D_2 (red) partial pressures measured with the optical Penning gauge during a 2 sec. long ECRH pulse (orange bar) and in post-discharge.

The amount of released D_2 was found to strongly depend on the ECRH power and amplitude of the vertical field, as it can be seen in FIG. 8 (a) and (b). However, as discussed above, B_V alone did not allow wetting inboard wall surfaces and resulted with strongest plasma wall interaction in the divertor area. Weak dependency on He inlet pressure was found, though highest release seemed to occur at lowest pressure (FIG. 8 (c)). Given the dependency of the breakdown time t_{Bd} on power and pressure, most of the discharges were therefore operated at p = 10^{-2} Pa and P_{EC} = 320-480 kW. Under such conditions, no dependency of D_2 release on the amplitude of B_H when applied alone could be identified.

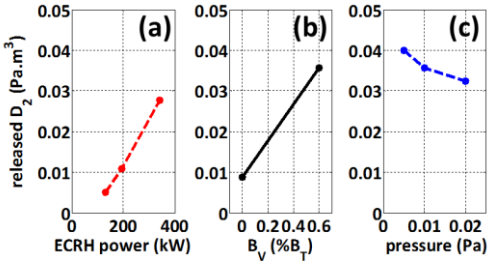

FIG. 8. Released D_2 as a function of ECRH power (a) B_V (b) and pressure (c).

Gas balance for all fifty-seven successful He-ECWC discharges operated in two experimental sessions in TCV is shown in FIG. 9, where the amount of D_2 (blue dots), of He (red), and their sum (pink) are integrated over the discharge and 60 sec. post-discharge durations for each shot, as discussed above.

The black dots in FIG. 9 are the integration of the total pressure in the Penning gauge, weighted by the relative content of D_2 and He molecules multiplied by their respective calibration factor (6 for He and 3 for D_2). In total, about $6.2 \cdot 10^{20}$ D_2 molecules could be removed. Half of this amount (0.6 Pa.m^3) was released from TCV walls during the first session, where thirty seven shots were executed. Despite this, the initiation ofa standard ohmic D_2-plasma could not be sustained at the end of the first session of He-ECWC (first non-sustained breakdown "nsb" in FIG. 9). During the second session, executed in three days, the same amount of D_2 could be recovered, but with twenty shots only.

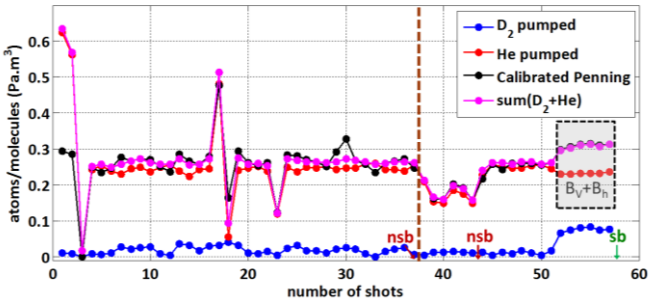

FIG. 9. Gas balance of the fifty seven He-ECWC discharges: released D_2 (blue), He (pink) and total amount (black and red) of gas and molecules

At the end of the second day, an attempt to initiate standard ohmic D_2-plasma resulted in the second non-sustained breakdown (second "nsb" in FIG. 9). Following this and the execution of the last fourteen He-ECWC discharges, an ohmic D_2-plasma could be successfully sustained, whereas it would not have been possible without conditioning. The last six He-ECWC discharges with optimized combinations of vertical and horizontal magnetic fields allowed recovering 75% (0.45 Pa.m^3) of the fuel in the second session. Moreover, gas balance indicated that 4% of the He injected was on the average retained in the carbon walls in these shots.

FIG. 10 shows the plasma current (a) and the line-averaged density (b) measured in three ohmic D_2-plasmas. The blue curves (shot 51926) stand for the plasma operated after 30 min. He-GDC during day 2 in the second ECWC experimental session, whereas the green curves (shot 51931) are those measured in a non-sustained breakdown at the end of the same day (second "nsb" in FIG. 9). The red curves are those of the plasma successfully initiated after the last fourteen He-ECWC discharges of FIG .9. Though the ability of ECWC, operated in X2 mode, to recover ohmic plasma has been hence demonstrated, FIG. 10 (b) obviously indicates a higher density in shot #51926 than in #51962, this for identical density requests and similar current ramp-ups in both shots. Similarly, D_α signal intensity in the ohmic plasmas was higher after ECWC than after GDC. It is therefore fair to say that the fourteen He-ECWC discharges, with 28 sec. long cumulated duration of applied EC power, did not allow complete density control in the ohmic plasma operated afterwards.

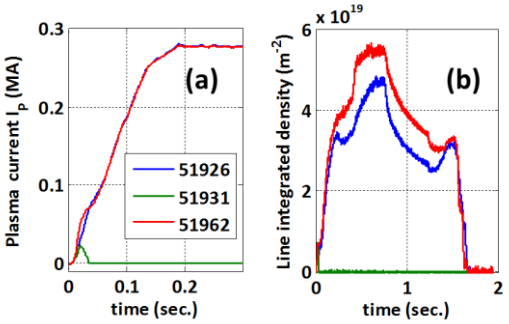

FIG. 10. Current (a) and density (b) in an ohmic D_2-plasma (Ip = 280 kA, B_T = 1.43 T) after He-GDC (blue), before (green) and after (red) He-ECWC.

4. Discussion and conclusion

Safe and efficient operation of ECWC requires paying attention to two aspects. Firstly, the discharge breakdown time has to be minimized in these optically thin plasmas in order to minimize absorption by in-vessel components of stray radiation at the onset of the discharge. Secondly, best homogeneity and largest wall coverage are needed to maximize fluxes of He^+ ions to the walls and hence conditioning efficiency. The conditions to fulfil both have been searched and met in ECWC discharges operated in TCV using optimized combinations of

vertical and radial magnetic fields. Application of the horizontal field is necessary to expand the discharge radially, but the operational space is limited to low amplitudes of B_H alone (0.2% of B_T in the present case), above which breakdown is too slow or simply not possible. A vertical field is therefore needed in order to minimize breakdown time and increase both plasma homogeneity and density, thus enhancing plasma production and enlarging operational space for the application of B_H.

In TCV, and *a fortiori* in JT-60SA, complete density control with He-ECWC would certainly require longer operation time, and to investigate a larger operational domain, e.g. with improved field patterns. However, given the high electron densities (up to $15 \cdot 10^{18}$ m^{-3}) and temperatures (20-40 eV) in ECWC plasmas, wall desorbed fuel is almost completely re-ionized and re-implanted, and only a small fraction of the released fuel is exhausted [11]. Even with the cryogenic pumping systems envisioned in JT-60SA (100 $m^3 \cdot s^{-1}$ in the divertor [12]), pulsed operation of ECWC may be mandatory to mitigate re-implantation of desorbed fuel, at the price of a reduction of the duration of the active phase of the discharge.

The conditioning efficiency of He-ECWC plasmas at second harmonic remains therefore to be demonstrated for an application to the operation of JT-60SA. Its ability to efficiently clean wall surfaces for reliable plasma initiation or recovery from disruption has still to be established. As reported in [7], conditioning efficiency is lower in X2 than in X1-mode. Therefore, in addition to the 110 and 138 GHz frequencies foreseen in JT-60SA, development aiming at short pulse operation at 82 GHz, using the same gyrotron, is on-going, and 1 MW output for 0.2 and 1 s with a duty cycle of 1/100 for 220 sec. was recently successfully achieved. The result is promising for wall conditioning using fundamental harmonic EC waves in JT-60SA, with the cold resonance layer located at R = 2.30 m for B_T = 2.25 T.

Acknowledgements

This work has been carried out within the framework of the EUROfusion Consortium and has received funding from the Euratom research and training programme 2014-2018 under grant agreement No 633053. The views and opinions expressed herein do not necessarily reflect those of the European Commission. The authors gratefully acknowledge members of the JT-60SA Integrated Project Team for data exchange and fruitful discussions.

References

[1] JT-60SA Research Plan
[2] T. Arai et al., J. Nuclear Materials 145-147 (1987) 686-690
[3] Y. Kobayashi et al., Proc. of the 21st IEEE/NPS Symposium on Fusion Engineering SOFE 05, Sept 25-29, 2005, Knoxville, TN, USA
[4] K. Itami et al., J. Nucl. Mat. 390–391 (2009) 983–987
[5] A. Lyssoivan et al., Proc. of the 14th Topical Conference on Radio Frequency Power in Plasmas, May 7-9, 2001, Oxnard, California, USA, Paper A34
[6] K. Itami et al., J. Nucl. Mat. 438 (2013) S930–S935
[7] M. Fukumoto et al., "Efficiency improvement by application of horizontal magnetic fields for second- and fundamental harmonic EC wall conditioning in JT-60U", submitted to Nuclear Materials and Energy
[8] D. Farina, Fusion Science and Technology, 52 (2007) 154-160
[9] A. Moro et al., "Electron Cyclotron stray radiation detection and machine protection system proposal for JT-60SA", Proc. of the 29th edition of the Symposium on Fusion Technology (SOFT 2016), Sept 5-9, 2016, Prague, Czech Republic
[10] J. Stober et al., Nucl. Fusion 51 (2011) 083031 (9pp)
[11] D. Douai et al., Journal of Nuclear Materials 415 (2011) S1021– S1028
[12] Y. Kamada et al., Nucl. Fusion 51 (2011) 073011 (11pp)